Electronic Supporting Information

Reversible inter-conversion of copper(II) dimers bearing phenolate–based ligands into their monomers: Theoretical and Experimental Visions

Pratibha Agarwal [a,#], Akhilesh Kumar [b,#], Richa [a], Indresh Verma [b], Rohan D. Erande [c], Julia Klak*[, d], Antonio J. Mota*[, e], Amit Rajput*[, a], and Himanshu Arora *[, a]

[a]*School of Engineering and Sciences, G.D. Goenka University, Gurugram, India. E-mail: himanshuiitk2004@gmail.com,+91 8860185079.*

[b] *Department of Chemistry, Indian Institute of Technology Kanpur, Kanpur 208 016, India*

[c] *Indian Institute of Technology Jodhpur, Jodhpur 342037, India.*

[d] *Faculty of Chemistry, University of Wroclaw, Wroclaw 50-383, Poland.*

[e]*Department of Inorganic Chemistry, Faculty of Science, University of Granada, 18071, Granada, Spain.*

[f]*Department of Chemistry, Axis Institute of Technology & Management Kanpur, Kanpur, India*

[#]*Both the authors have equal contribution.*

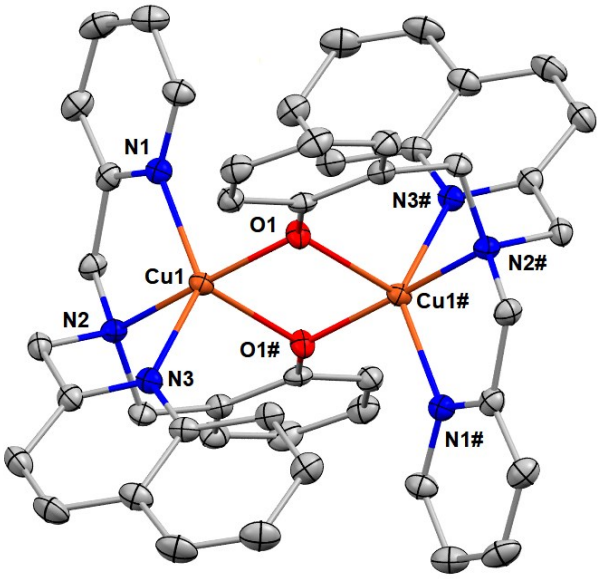

Fig. S1 Perspective view of the structure of $[Cu_2(L^2)_2](ClO_4)_2 \bullet CH_3CN$ (**2**). Only donor atoms are labeled. All the hydrogen atoms are omitted for clarity.

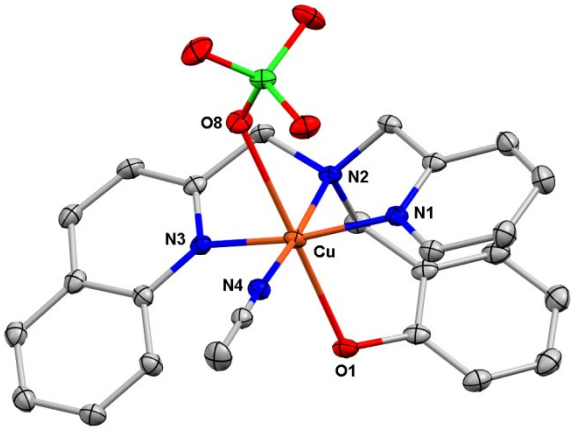

Fig. S2 Perspective view of the structure of $[Cu(HL^2)(NCCH_3)(OClO_3)](ClO_4)\bullet CH_3CN$ (**4**). Only donor atoms are labeled. All the hydrogen atoms are omitted for clarity.

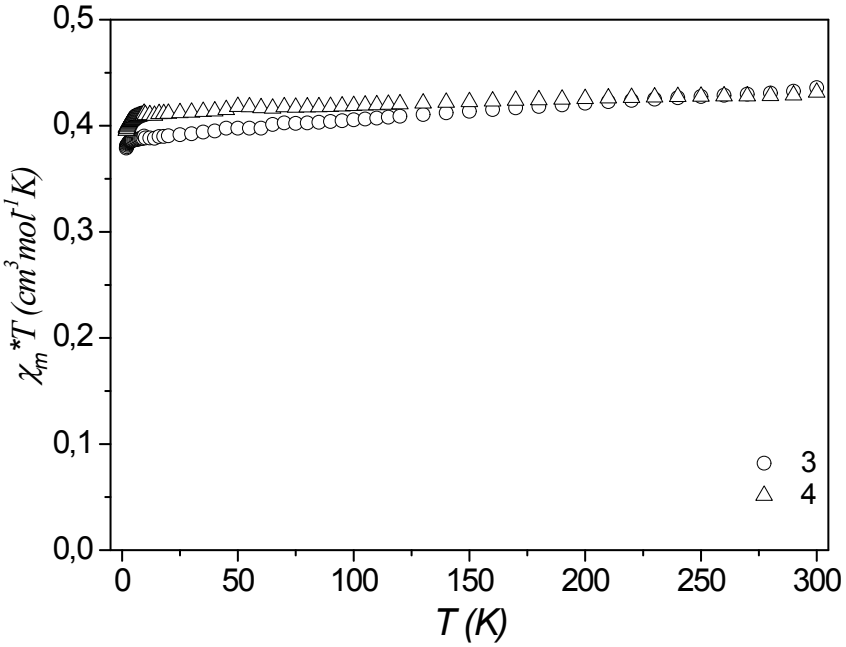

Fig. S3 Temperature dependence of experimental $\chi_m T$ (χ_m per 1 Cu^{II} atom) for **3** and **4**.

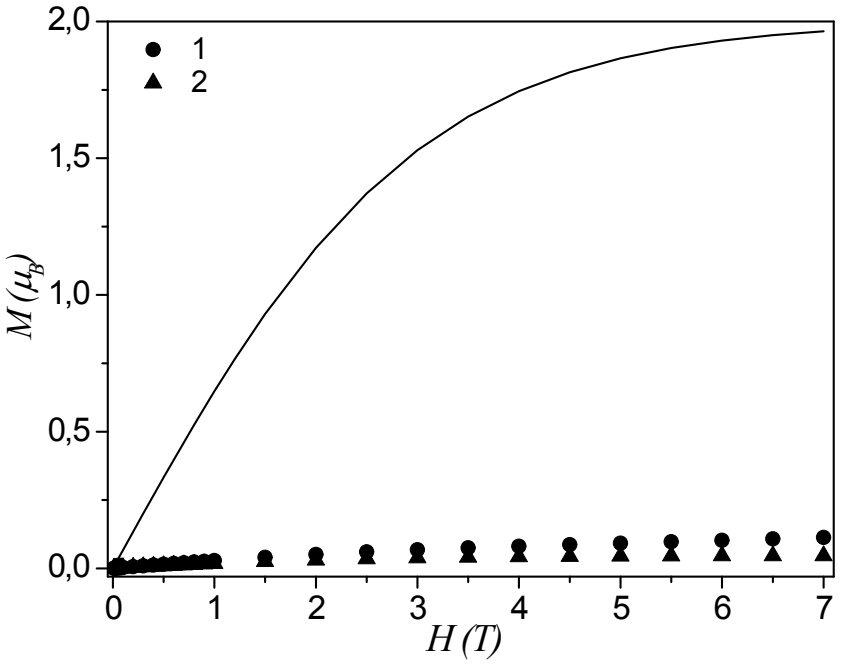

Fig. S4 Field dependence of the magnetization (*M* per Cu_2 entities) for **1** and **2**. The solid line is the Brillouin function curve for the system of two uncoupled spins with $S = {}^1/_2$ and $g = 2.0$.

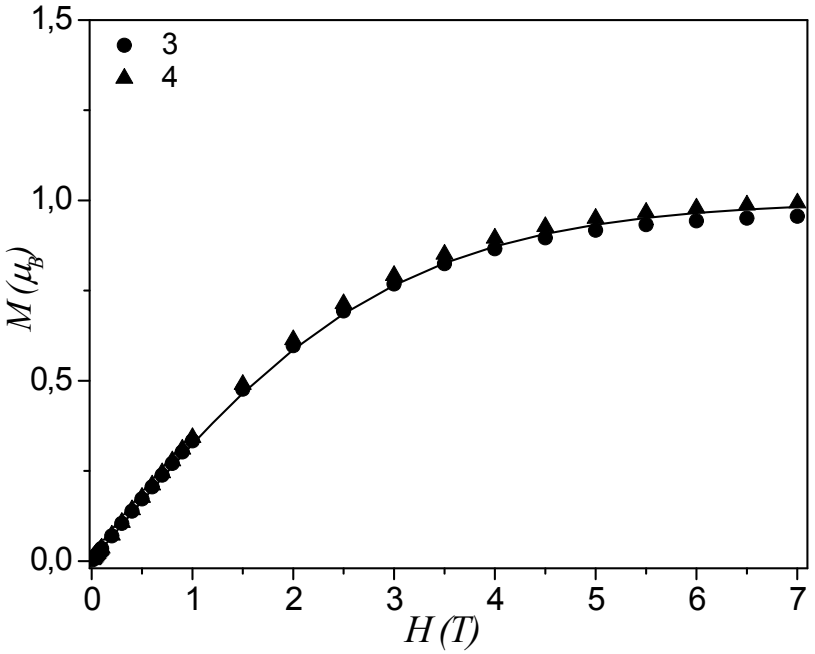

Fig. S5 Field dependence of the magnetization (*M* per 1 Cu^{II} atom) for **3** and **4**. The solid line is the Brillouin function curve for one uncoupled spin with $S = {}^1/_2$ and $g = 2.0$.

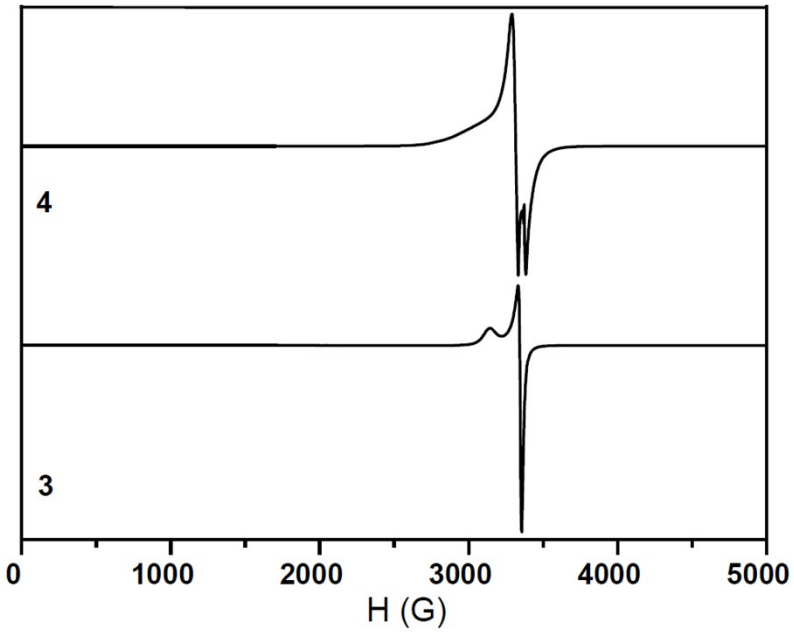

Fig. S6 EPR (X-band) spectra of powdered samples **3** and **4** at 77 K.

Table S1. Selected Bond Lengths (Å), and Angles (°) in $[Cu_2(L^1)_2](ClO_4)_2$•$2CH_3CN$ (**1**), $[Cu_2(L^2)_2](ClO_4)_2$•CH_3CN (**2**), $[Cu(HL^1)(NCCH_3)](ClO_4)_2$ (**3**) and $[Cu(HL^2)(NCCH_3)(OClO_3)](ClO_4)$•$CH_3CN$ (**4**).

1			
N(3)–Cu–N(2)#	83.9(2)	N(3)–Cu–N(1)#	144.4(2)
N(2)–Cu–O(1)#	91.09(19)	N(1)–Cu–O(1)#	102.4(2)
N(1)–Cu–N(2)#	80.1(2)		
# [1–x, 1–y, 1–z]			
2			
Cu(2)–O(2)	1.9270(18)	N(1)–Cu(1)–N(3)#	134.83(9)
Cu(2)–O(2)$	2.1074(19)	N(2)–Cu(1)–O(1)#	92.09(8)
Cu(2)–N(4)	2.014(2)	N(2)–Cu(1)–N(1)#	82.64(9)
Cu(2)–N(5)	2.003(2)	N(2)–Cu(1)–N(3)#	80.95(9)
Cu(2)–N(6)	2.088(2)	N(3)–Cu(1)–O(1)#	104.76(8)

Cu(2)···Cu(2)$	3.0946(6)	N(4)–Cu(2)–N(6)$	137.65(9)
		N(5)–Cu(2)–O(2)$	92.04(8)
		N(5)–Cu(2)–N(6)$	82.32(9)
		N(6)–Cu(2)–O(2)$	109.05(8)
		N(5)–Cu (2)–N(4)$	83.09(9)
		Cu(2)–O(2)–Cu(2)	100.09(8)
# [1–x, 1–y, 1–z], $ [1–x, 1–y, 2–z]			
3			
N(4)–Cu–O(1)	106.34(12)	N(3)–Cu–N(4)	82.13(13)
N(5)–Cu–O(1)	87.06(12)	N(3)–Cu–N(5)	176.19(13)
N(4)–Cu–N(5)	94.95(13)		
4			
N(4)–Cu–O(1)	96.97(7)	N(3)–Cu–N(4)	100.29(8)
N(2)–Cu–O(1)	90.53(7)	N(2)–Cu–N(3)	81.77(8)
N(2)–Cu–N(4)	172.16(8)		

Table S2. Spin density values for selected atoms on complexes **1** and **2**.

Complex	**1**	**2a**	**2b**
Cu[a]	0.6290	0.6221	0.6213
O_{bridge}[b]	0.0977	0.0861	0.0785
$N_{im/quin}$[b]	0.0683	0.0491	0.0426
N_{tert}[b]	0.1205	0.1328	0.1372
N_{py}[b]	0.0654	0.0739	0.0753

[a] Only a half of each structure is shown because they are centrosymmetric. All values on the same half have the same sign and opposite sign with respect to the other half. [b] Directly attached atoms in the magnetic orbital plane: O_{bridge} is the oxygen bridging atom in the magnetic orbital plane, $N_{im/quin}$ is the imidazolic nitrogen atom in complex **1** and quinolinic in complex **2**, N_{tert} is the aminic, tertiary nitrogen atom, and N_{py} corresponds to the pyridinic nitrogen atom.

Table S3. Absorption spectra of the metal complexes in CH_3CN solution

Complex	λ_{max}/nm (ε/M^{-1} cm^{-1})
$[Cu_2(L^1)_2](ClO_4)_2$•$2CH_3CN$ (**1**)	293 (17600), 460sh (560), 870 (600)
$[Cu_2(L^2)_2](ClO_4)_2$•CH_3CN (**2**)	320sh (9680), 460sh (390), 870 (370)
$[Cu(HL^1)(NCCH_3)](ClO_4)_2$ (**3**)	272 (17200), 615 (120)
$[Cu(HL^2)(NCCH_3)(OClO_3)](ClO_4)$•$CH_3CN$ (**4**)	320sh (8500), 615 (130)
$[CuL^1(py)]^+$	470 (700), 730 (250)
$[CuL^2(py)]^+$	470 (1150), 660 (350)
HL^1	287 (25000), 290 (12000)
HL^2	302 (15000), 315 (17000)

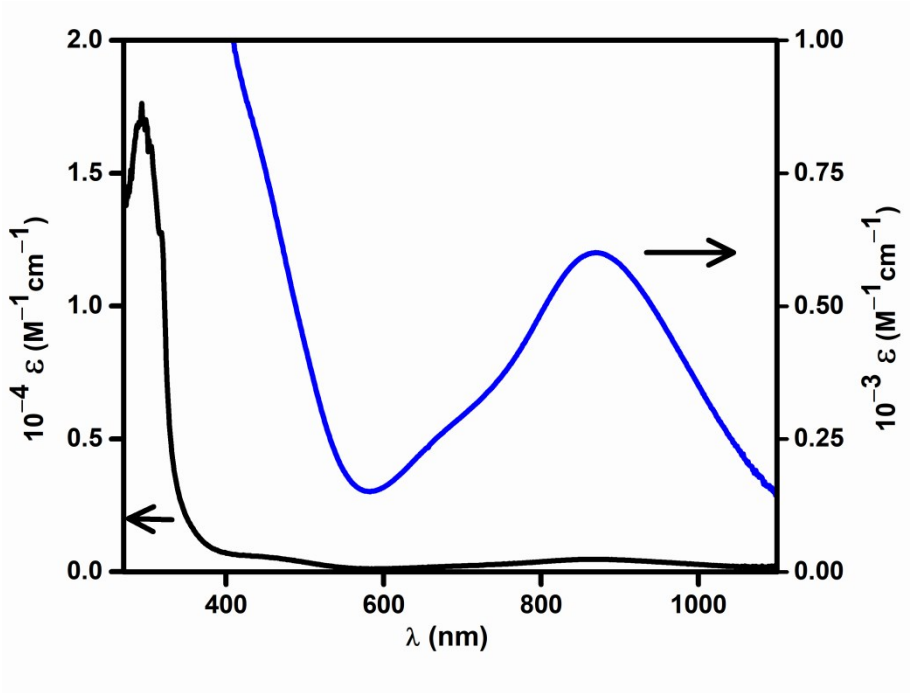

Fig S7. UV-Vis of $[Cu_2(L^1)_2](ClO_4)_2$•$2CH_3CN$ (**1**) in CH_3CN

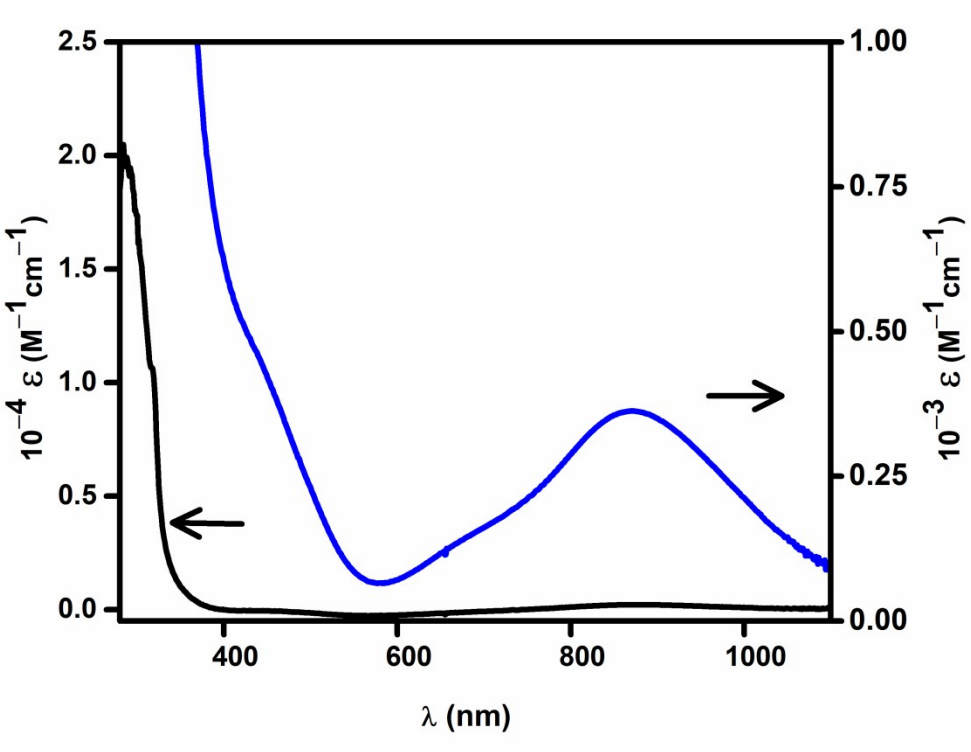

Fig S8. UV-Vis of $[Cu_2(L^2)_2](ClO_4)_2 \bullet CH_3CN$ (**2**) in CH_3CN

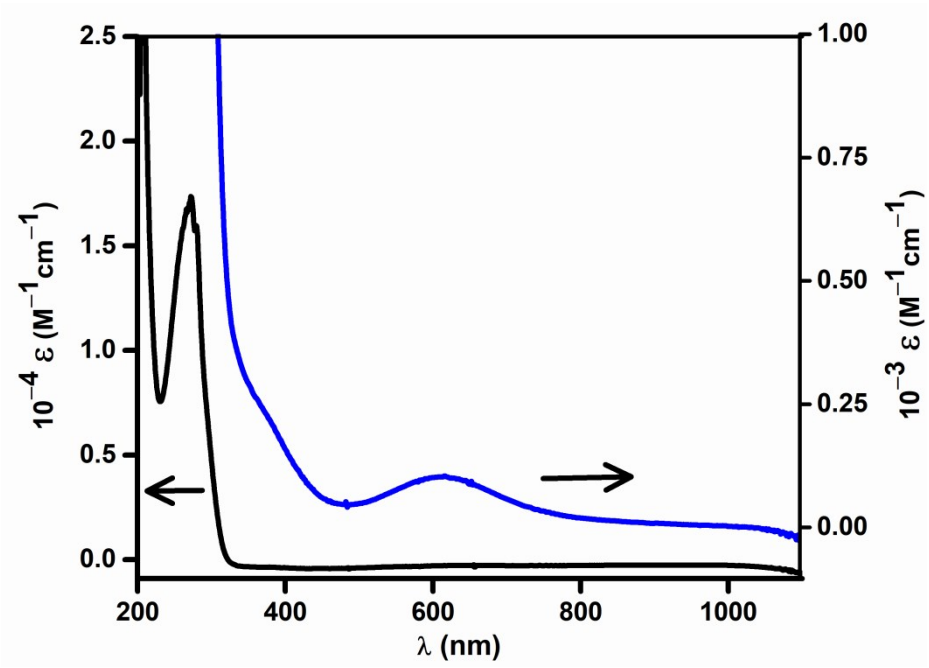

Fig S9. UV-Vis of $[Cu(HL^1)(NCCH_3)](ClO_4)_2$ (**3**) in CH_3CN

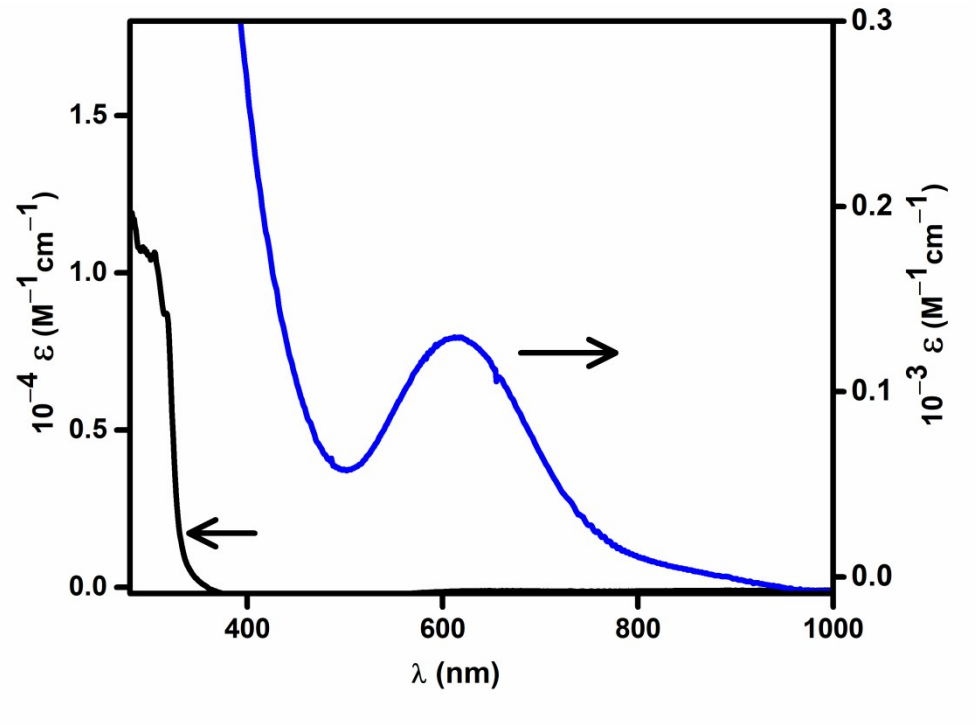

Fig S10. UV-Vis of $[Cu(HL^2)(NCCH_3)(OClO_3)](ClO_4)\bullet CH_3CN$ (**4**) in CH_3CN

(a) (b)

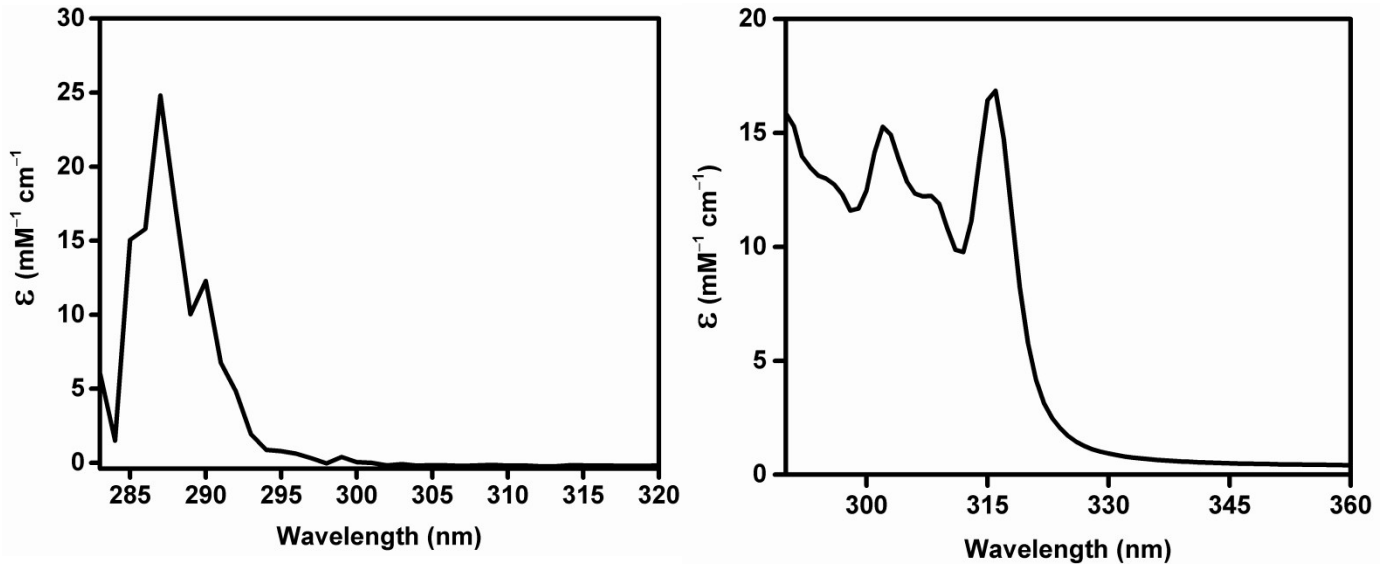

Fig S11. UV-Vis of (a) HL^1 and (b) HL^2 in CH_3CN

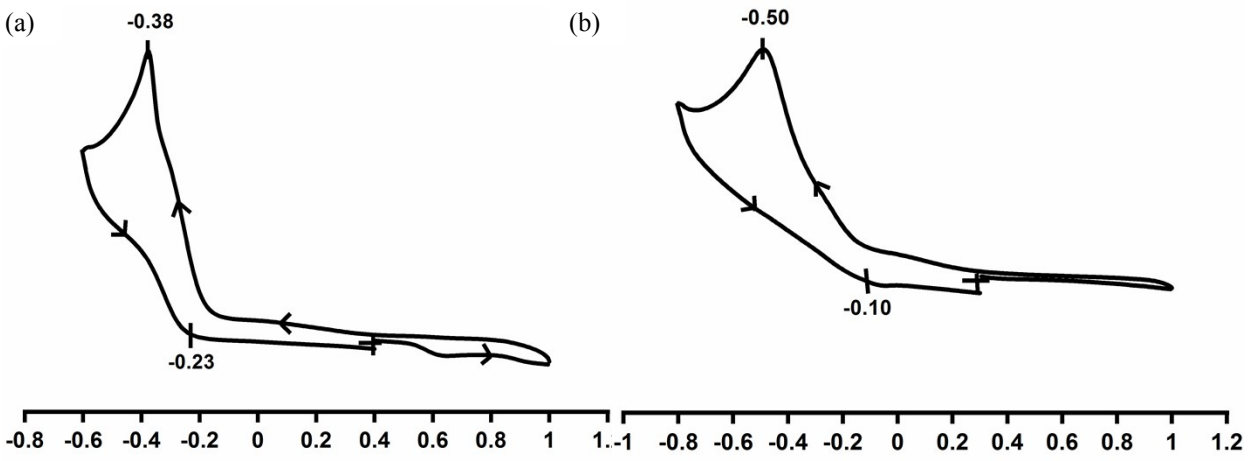

Fig. S12 Cyclic voltammogram (100 mV/s) of 1 mM solution of (a) **1** at GC electrode and (b) **2** at platinum electrode in CH_3CN (0.1 M in TBAP). Indicated peak potentials are in V *vs.* Ag^+/AgCl.

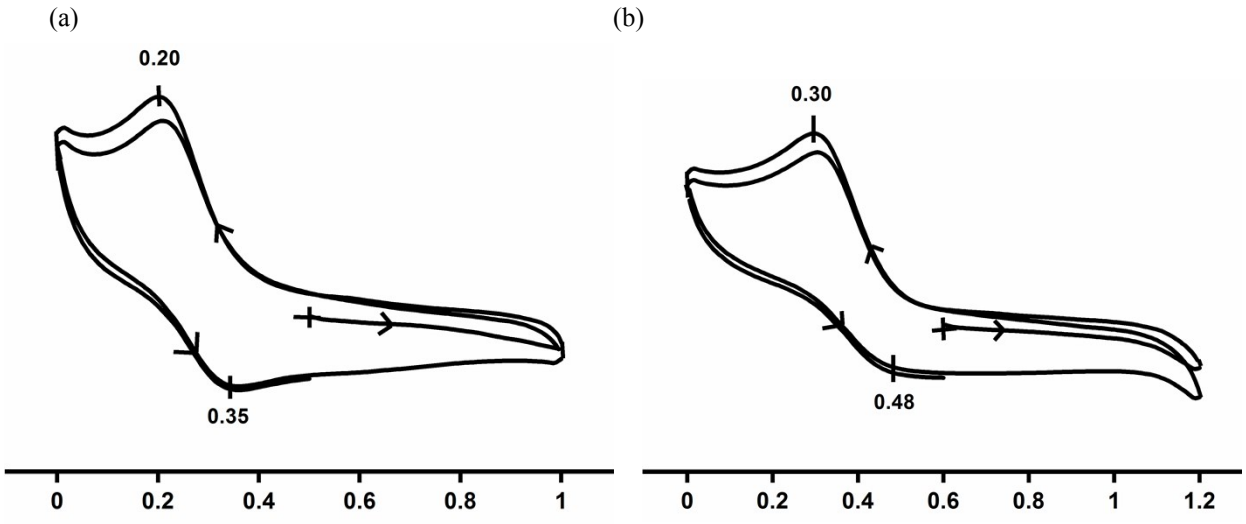

Fig. S13 Cyclic voltammogram (100 mV/s) of 1 mM solution of (a) **3** at GC electrode and (b) **4** at platinum electrode in CH_3CN (0.1 M in TBAP). Indicated peak potentials are in V *vs.* Ag^+/AgCl.

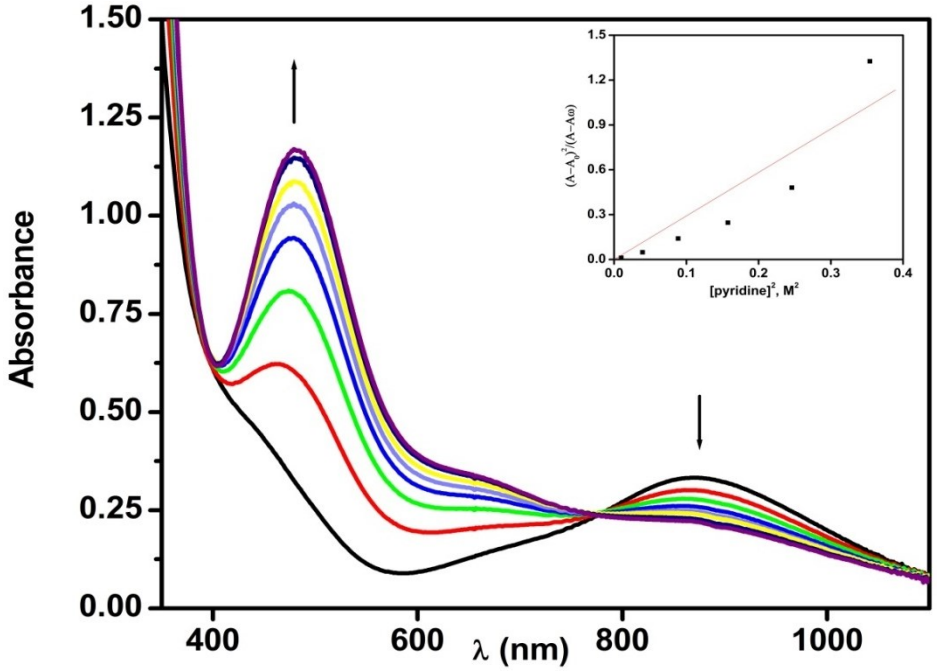

Fig. S14 Spectral change of the titration of $[Cu_2L^2_2]$ (1.0×10^{-3} M) by pyridine (0 – 0.004 M) in CH_3CN. Inset: plot of $(A - A_o)^2/(A - A_\infty)$ vs. [pyridine]$_2$ for the titration. Black line: $[Cu_2L^1_2]^{2+}$ and other lines: $[Cu_2L^1_2]^{2+}$ with incremental addition of pyridine.

(a) (b)

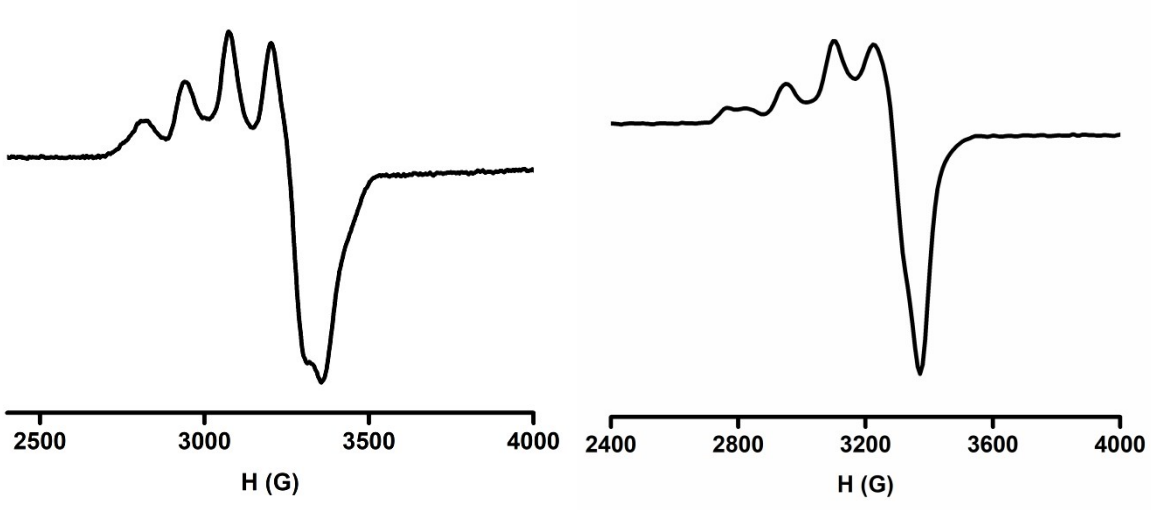

Fig. S15 ESR spectra of (a) $[CuL^1(py)]^+$ and (b) $[CuL^2(py)]^+$ generated from the dimer (10^{-3} M) by adding pyridine (4×10^{-3} M) in CH_3CN at 120 K; microwave frequency 9.414 GHz, modulation frequency 100 kHz, modulation amplitude 5 G, microwave power 6.31 mW.

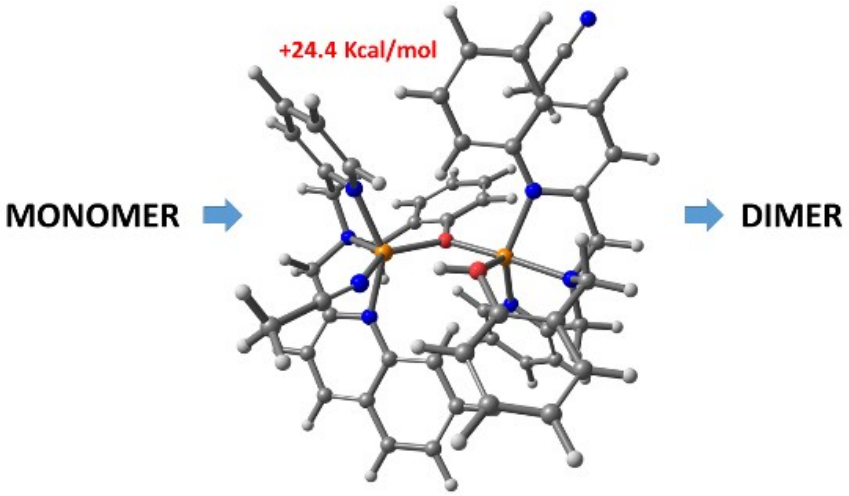

Fig. S16 Schematic pathway for the monomer to dimer conversion for the thermodynamic process: $2Et_3N + 2[CuL^2(CH_3CN)]^{2+}$ (monomer) → $Et_3N + Et_3NH^+$ + Dimeric intermediate → $2Et_3NH^+ + [Cu_2L^2_2]^{2+}(CH_3CN)_2$ (dimer).

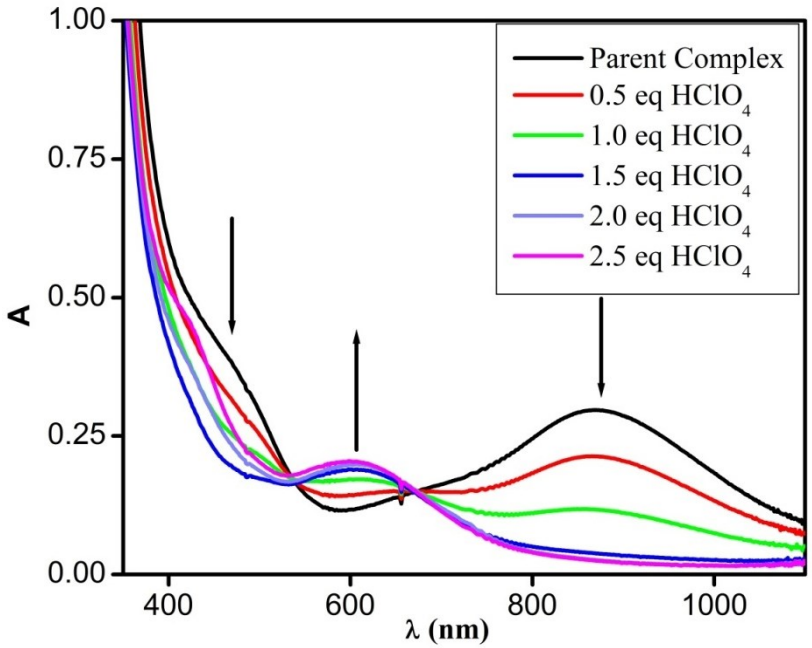

Fig. S17 Spectral change of the titration of $[Cu_2L^2_2](ClO_4)_2$ (1.0×10^{-3} M) by $HClO_4$ (0–2.5 eq.) in CH_3CN.

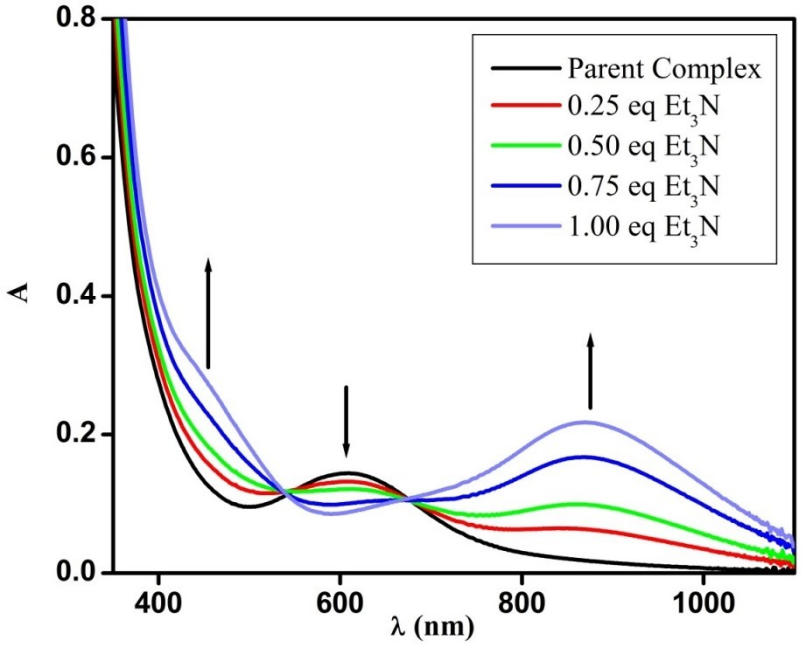

Fig. S18 Spectral change of the titration of $[CuL^2(CH_3CN)(OClO_3](ClO_4)$ (1.0×10^{-3} M) by Et_3N (0–1 eq.) in CH_3CN.